Bioconjugate Chemistry

Article

pubs.acs.org/bc

Synthesis and Characterization of Pt(IV) Fluorescein Conjugates to Investigate Pt(IV) Intracellular Transformations

Ying Song,[†] Kogularamanan Suntharalingam,[†] Jessica S. Yeung, Maksim Royzen,[†] and Stephen J. Lippard*,[†]

[†]Department of Chemistry, Massachusetts Institute of Technology, Cambridge, Massachusetts 02139, United States

Supporting Information

ABSTRACT: Pt(IV) anticancer compounds typically operate as prodrugs that are reduced in the hypoxic environment of cancer cells, losing two axial ligands in the process to generate active Pt(II) species. Here we report the synthesis of two fluorescent Pt(IV) prodrugs of cisplatin in order to image and evaluate the Pt(IV) reduction process in simulated and real biological environments. Treatment of the complexes dissolved in PBS buffer with reducing agents typically encountered in cells, glutathione or ascorbate, afforded a 3- to 5-fold fluorescence turn-on owing to reduction and loss of their fluorescein-based axial ligands, which are quenched when bound to platinum. Both Pt(IV) conjugates displayed moderate cytotoxicity against human cancer cell lines, with IC_{50} values higher than that of cisplatin. Immunoblotting and DNA flow cytometry analyses of one of the complexes, Pt(IV)FL_2, revealed that it damages DNA, causes cell cycle arrest in S or G2/M depending on exposure time, and ultimately triggers apoptotic cell death. Fluorescence microscopic studies prove that Pt(IV)FL_2 enters cells intact and undergoes reduction intracellularly. The results are best interpreted in terms of a model in which the axial fluorescein ligands are expelled through lysosomes, with the platinum(II) moiety generated in the process binding to genomic DNA, which results in cell death.

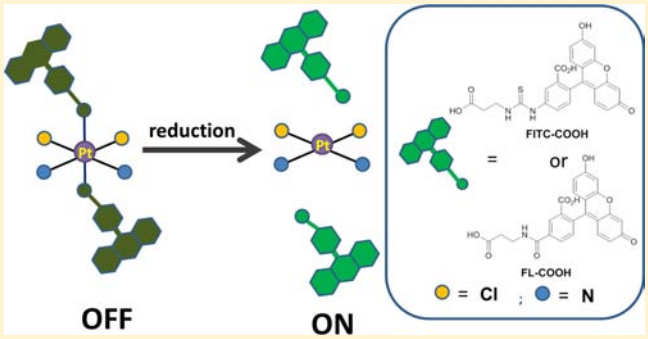

INTRODUCTION

Cisplatin and other platinum-based anticancer drugs are widely used to treat cancer, including testicular, head and neck, prostate, ovarian, breast, and lung.[1,2] Acquired resistance and unpleasant side effects, however, have prompted the investigation of Pt(IV) complexes as an alternative for safer and more effective delivery of platinum.[3−5] Many octahedral Pt(IV) prodrugs have been reported with axial ligands designed to optimize physical, redox, and/or pharmacokinetic properties.[6−9] Nevertheless, owing to their suboptimal efficacy, only a few Pt(IV) compounds have entered, or are under consideration for, clinical trials.[2,10,11] A better understanding of their molecular mechanisms of action is necessary in order to generate potent Pt(IV) complexes with improved clinical outcomes.

Several Pt(IV) compounds in biological environments have been studied using elemental imaging techniques, such as electron microscopy, X-ray fluorescence, X-ray absorption near-edge spectroscopy (XANES), and micro-XANES.[5,12−14] Based on the results of these investigations, a general mechanism has been proposed in an attempt to unify the Pt(IV)-based prodrug approach, as illustrated in Figure 1.[15] Pt(IV) compounds are considered to be kinetically inert. They can enter cancer cells either intact or following reduction by extracellular agents, such as glutathione or ascorbate. Reduction of Pt(IV) can also occur inside the cell, resulting in square-planar Pt(II) compounds after the loss of two axial ligands. The active Pt(II) species can then enter the nucleus and bind to genomic DNA.

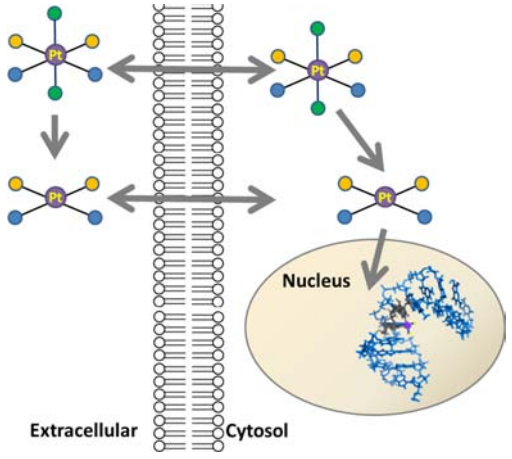

Figure 1. Schematic illustration of Pt(IV) prodrug activation in a cellular environment.

Received: June 12, 2013
Revised: August 11, 2013
Published: August 20, 2013

Fluorescence imaging can provide a quantitative readout of dynamic processes that occur in live cells.[16] In this respect, a Pt(IV)/Pt(II) redox-sensitive optical probe would be valuable for improving our understanding of the biotransformation of Pt(IV) prodrugs. Specifically, a fluorescent probe sensitive to the oxidation state of platinum could be used to study cellular uptake, subcellular localization, and the kinetics of intracellular prodrug reductive activation. A small number of fluorescently labeled Pt(IV) compounds have recently been described in the literature.[17−20] Notably, none of these compounds have been successfully used in live cell imaging to monitor Pt(IV) reduction. The present work attempts to fill this void by introducing two new fluorescent Pt(IV) complexes that can serve as reporters of prodrug activation in live cell imaging studies.

Here, we present the design and synthesis of two prodrugs of cisplatin, Pt(IV)$(FITC)_2$ and Pt(IV)FL_2 (Scheme 1). These Pt(IV)-conjugates have been used to image the transformation of Pt(IV) to Pt(II), a key step in Pt(IV) prodrug activation. Both probes contain fluorescein, an effective fluorescent reporter frequently applied in live cell imaging. Fluorescein was chosen because it (i) is nontoxic, (ii) displays excellent photophysical properties and gives good contrast against the background in cellular studies, (iii) can be readily synthesized on the gram-scale, and (iv) is routinely used in cell imaging and allows common filter sets to be used. In the parent Pt(IV) complexes, two fluorescein molecules are held in close proximity at opposing axial positions. This disposition of fluorescein groups was chosen based on the expectation of diminished luminescence, an OFF-state, owing to quenching through homo fluorescence resonance energy transfer (homo-FRET).[21] The heavy metal effect can also contribute to quenching.[22] The intracellular reduction of Pt(IV) to Pt(II) is envisaged to release the two axial fluoresceins and consequently restore their fluorescence (ON-state), as depicted in Scheme 1. Pt(IV)$(FITC)_2$ and Pt(IV)FL_2 are fluorescence probes that turn on upon activation. There are several advantages of such probes over conventional "always-on" probes. For instance, probes that can be activated will (i) turn on under specific conditions triggered by a specific biological event and (ii) display superior sensitivity over conventional probes because the signal is maximized upon activation while the background is minimized.

Scheme 1. Illustration of the Fluorescence 'Turn-on' of the Pt(IV) Complexes Described in This Work Following Reduction of Platinum and Release of the Axial Fluorescein Ligands

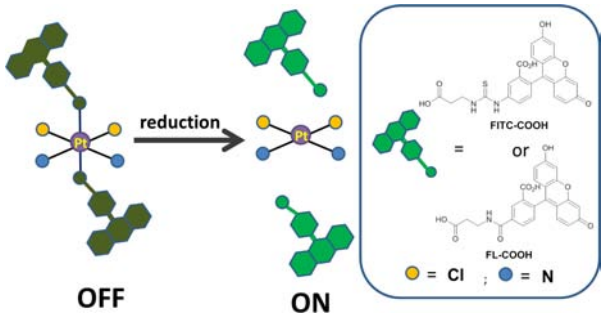

RESULTS AND DISCUSSION

Synthesis of Fluorescein Conjugated Pt(IV) Complexes. The desired Pt(IV) compounds were prepared in four steps. In the first step, cisplatin was oxidized with H_2O_2 to form *c,c,t*-$[PtCl_2(NH_3)_2(OH)_2]$, **1**.[5] Compound **1** was then allowed to react with *N*-Boc aminopropanoic acid anhydride, **2**,

Scheme 2. Preparation of Pt(IV)FL_2 and Pt(IV)$(FITC)_2$[a]

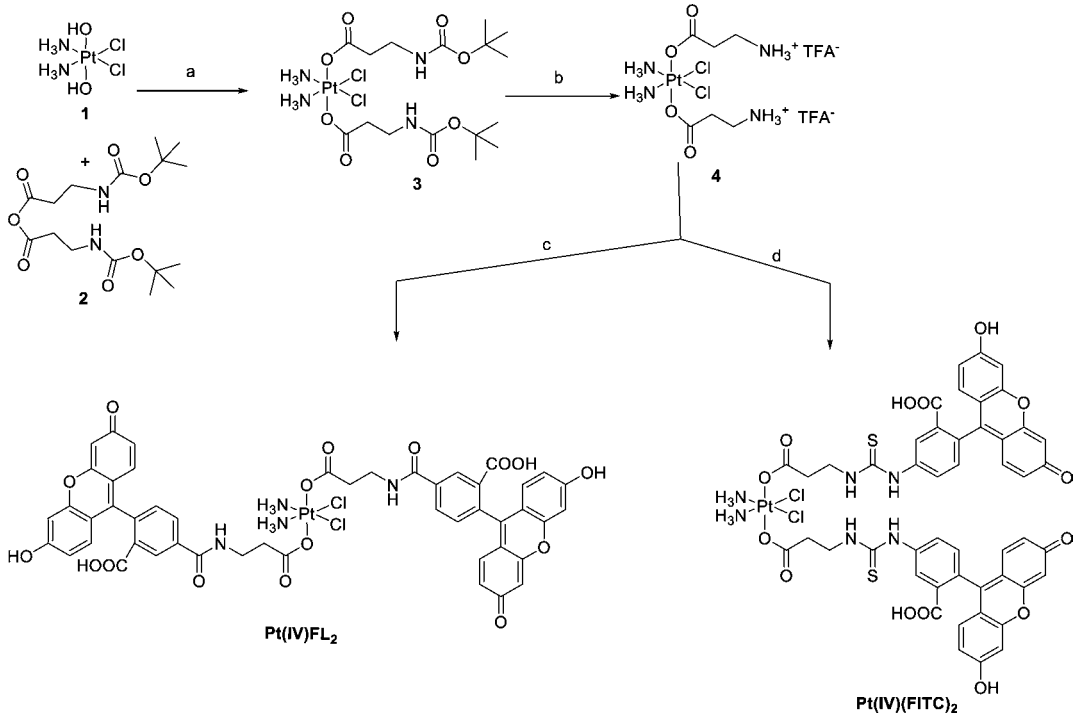

[a]Conditions: (a) DMF, 50 °C; (b) trifluoroacetic acid/dichloromethane; (c) fluorescein-NHS, DIPEA, DMF; (d) FITC, DIPEA, DMF.

dx.doi.org/10.1021/bc400281a | Bioconjugate Chem. 2013, 24, 1733−1740

to yield **3** (Scheme 2). The Boc protecting groups were removed using trifluoroacetic acid to generate compound **4** with two terminal amino groups in the axial positions. The pendant amino groups were then used to introduce either thiourea or amide linkages to fluorescein, forming Pt(IV)-$(FITC)_2$ or $Pt(IV)FL_2$. Specifically, $Pt(IV)(FITC)_2$ was prepared by treating **4** with fluorescein isothiocyanate (FITC), whereas $Pt(IV)FL_2$ was synthesized by coupling **4** with fluorescein NHS ester. Both Pt(IV) compounds exhibit poor water solubility. Concentrated solutions were therefore prepared in DMF and diluted with aqueous buffer immediately prior to all photophysical measurements and biological studies.

Photophysical Properties. We chose, as fluorescein axial ligands, FITC−COOH and FL−COOH in order to compare their absorption and fluorescence properties when attached to the Pt(IV) center and after reduction-triggered release (Scheme 1). The photophysical properties of the Pt(IV) complexes and the corresponding axial ligands were measured in pH 7.4 PBS buffer at 25 °C. The results are listed in Table 1. The

Table 1. Photophysical Properties of $Pt(IV)(FITC)_2$ and $Pt(IV)FL_2$ and Their Corresponding Free Axial Ligand FITC−COOH and FL−COOH (25 °C, PBS buffer)

	absorption λ_{max} (nm)	$\varepsilon \times 10^5$ (M^{-1} cm^{-1})	emission λ_{max} (nm)[a]	quantum yield
Pt(IV) $(FITC)_2$	493	2.63	520	0.29
FITC−COOH	493	1.30	520	0.77
$Pt(IV)FL_2$	493	2.91	520	0.32
FL-COOH	493	1.45	520	0.90
fluorescein[a]	490	7.69	521	0.93[24]

[a]Excitation wavelength, 493 nm.

absorption and emission spectra of FITC−COOH and FL−COOH are characteristic of the fluorescein chromophore. Both axial ligands have an absorbance maximum at 493 nm and a strong fluorescence emission signal at 520 nm. The fluorescence quantum yields, measured by using fluorescein as a standard, are 0.77 for FITC−COOH and 0.90 for FL−COOH. The additional carboxylate group has minimal effect on the emission properties of fluorescein.

The extinction coefficients of $Pt(IV)(FITC)_2$ and $Pt(IV)FL_2$ are approximately twice those of the corresponding axial ligands, which is consistent with the presence of two chromophores per Pt(IV) complex. On the other hand, the fluorescence quantum yields of the Pt(IV) complexes are more than 2.5-fold lower than those of the corresponding axial ligands. This partial fluorescence quenching is attributed to homo-FRET between the two chromophores.[23] We do not exclude the possibility of heavy metal quenching, which has been previously described for other Pt(IV) complexes.[19] Figure S1 (Supporting Information, SI) illustrates the overlap between excitation and emission spectra of $Pt(IV)(FITC)_2$, which is necessary for the homo-FRET quenching process to occur.

Influence of Reducing Agents on Fluorescence. The effects of two biologically relevant reducing agents, glutathione (GSH) and sodium ascorbate (Asc), on the fluorescence of $Pt(IV)(FITC)_2$ and $Pt(IV)FL_2$ were investigated under simulated physiological conditions (PBS, pH 7.4, 37 °C). The intracellular concentration of GSH is ∼0.5−10 mM, whereas plasma concentrations of this reducing agent are typically in the micromolar range (2−20 μM).[25] The plasma concentration of Asc is approximately 50 μM, and the intracellular concentrations are several orders of magnitude higher.[26,27] In an attempt to mimic biologically relevant concentrations, we studied the responses of 5 μM Pt(IV)-$(FITC)_2$ or $Pt(IV)FL_2$ to a 10- or 1000-fold excess of Asc or GSH. The fluorescence at 520 nm was observed as a function of time (Figures 2 and S2, and S3 in SI).

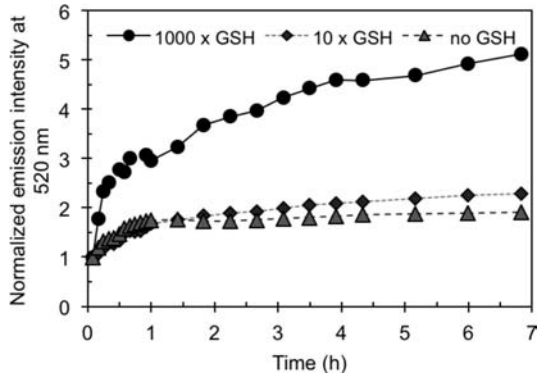

Figure 2. Fluoresence intensity at 520 nm of 5 μM $Pt(IV)FL_2$ in PBS, pH 7.4, at 37 °C following addition of varying concentrations of GSH (50 μM or 5 mM) over time. The data are an average of three independent determinations and the error associated with each point is <1%.

A 5-fold fluorescence turn-on occurred upon treatment of 5 μM $Pt(IV)FL_2$ with 5 mM GSH over a 7 h period. Based on quantum yields (Table 1), such a turn-on is consistent with the release of both axial ligands following Pt(IV) reduction. By comparison, FL-COOH did not show a fluorescence response to the addition of GSH (Figure S4). The release of the axial ligands was further confirmed by LC-MS analysis. A 100-fold excess of GSH or Asc was mixed with $Pt(IV)FL_2$ in PBS at pH 7.4 and the absorbance of the effluent was monitored at 490 nm. Over time, the $Pt(IV)FL_2$ peak decreased in the presence of GSH or Asc with half-lives of 2.0 and 1.2 h, respectively, whereas fluorescence due to the axial ligand FL-COOH increased (Figures S5, S6). When $Pt(IV)FL_2$ and 100 equiv of GSH were mixed in PBS without adjusting the pH to 7.4, no obvious peak corresponding to the formation of FL-COOH was observed. This result indicates that reduction of Pt(IV)-$(FITC)_2$ by GSH is pH-sensitive and that, under acidic conditions, Pt(IV) reduction by GSH is slow. Such retardation of the rate of reduction is most likely due to the protonation state of the thiol.

A small increase in fluorescence intensity was observed in PBS at pH 7.4 in the absence of any reducing agents, which depends on both pH and solution composition (Figure 3). At pH 7.4, there was a 1.8-fold increase of fluorescence in 6 h, whereas at pH 6.0 the increase was 1.2-fold. Under acidic conditions (sodium citrate buffer, pH = 4.5 and 5.5) there was minimal enhancement in emission, suggestive of acid mediated stability. This behavior was further investigated using LC-MS. In PBS at pH 7.4 the axial ligands of $Pt(IV)FL_2$ detach over the time period of 7 h, $t_{1/2}$ = 5.8 h (Figure S7). Remarkably, in Millipore water (pH ∼7) no obvious dissociation was observed over the same time period (Figure S8). The phenomenon of axial ligand hydrolysis in Pt(IV) complexes has been reported in recent literature.[28] Nonetheless, the dissociation rate of FL-COOH from $Pt(IV)FL_2$ in PBS, pH 7.4, was three to four times slower than that in the presence of a reducing agent, GSH or

dx.doi.org/10.1021/bc400281a | Bioconjugate Chem. 2013, 24, 1733−1740

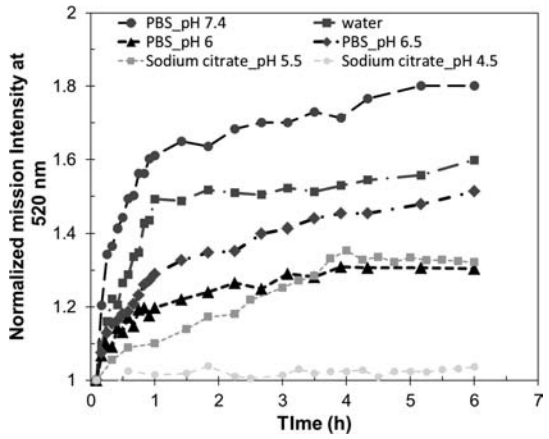

Figure 3. Fluorescence intensity of Pt(IV)$(FITC)_2$ at 520 nm over time in PBS buffer at pH values of 6.0, 6.5, and 7.4, sodium citrate buffer at pH values 4.5 and 5.5, and in unbuffered Millipore (pH ~7.0) water over time, at 37 °C. The data are an average of three independent determinations and the error associated with each point is <1%.

Asc, under the same conditions. It appears that reduction is essential for complete activation of the Pt(IV) compounds.

There are two possible mechanisms to account for the release of the axial ligands and concomitant increase in emission intensity, namely, ligand substitution and hydrolysis. Pt(IV) complexes are in general kinetically inert to ligand displacement by water or similar nucleophiles. Hydrolysis of an acetate ligand in the axial position of a Pt(IV) complex is determined by the Lewis acidity of the metal ion and can be facilitated by hydroxide ion under basic conditions through deprotonation of the equatorial ammines. Additional studies beyond the scope of this work are required to establish the mechanism.

In order to investigate the potential of the Pt(IV) compounds as live cell imaging and therapeutic agents, their stability was studied in culture medium (DMEM) and human plasma. Upon addition of Pt(IV)$(FITC)_2$ to DMEM or human blood plasma at a final concentration of 5 μM, an ~2.5-fold increase in fluorescence occurred over the course of 7 h (Figure 4). This enhancement can be attributed to reduction of Pt(IV) by agents such as L-cysteine, present in both solutions. However, the fluorescence enhancement is 2–3-fold lower

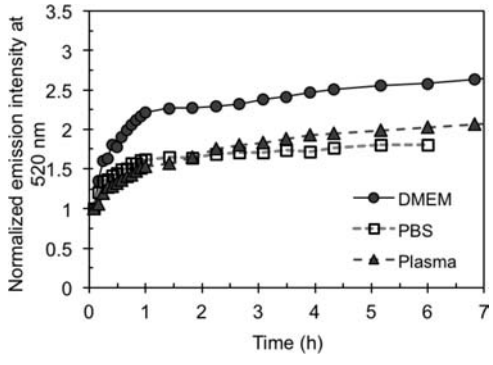

Figure 4. Fluorescence intensity of Pt(IV)$(FITC)_2$ at 520 nm over time in DMEM cell culture medium (without phenol red), or human plasma (1:4 dilution in PBS) in comparison to that in PBS, pH 7.4 at 37 °C. The data are an average of three independent determinations and the error associated with each point is <1%.

than that observed in the presence of biomimetic concentrations of exogenous GSH or Asc. Therefore, Pt(IV)$(FITC)_2$ is unlikely to undergo full reduction in DMEM or plasma and can be considered sufficiently stable for use in cellular studies.

Cytotoxicity Studies. The antiproliferative activities of Pt(IV)$(FITC)_2$, Pt(IV)FL_2, and cisplatin as a control were evaluated by MTT assays in the human cervical cancer cell line HeLa and human lung cancer cell line, A549. Table 2 summarizes the 50% growth inhibitory concentration (IC_{50}) values of these compounds, and Figure S9 shows representative dose–response curves. Pt(IV)$(FITC)_2$ and Pt(IV)FL_2 display similar toxicity profiles. Pt(IV)FL_2, however, is slightly more toxic than Pt(IV)$(FITC)_2$. Both complexes exhibit lower potency compared to cisplatin (10–20-fold). Overall, the IC_{50} values are analogous to those reported for other Pt(IV) compounds.[15] We do not expect the fluorescein moiety to cause cell toxicity in the μM range, so cell killing is likely to result from the activated Pt(II) species produced inside cells.

Table 2. IC_{50}/μM Values of Pt(IV) Compounds in Comparison to Those of Cisplatin[a]

cells	cell type	cisplatin	Pt(IV)$(FITC)_2$	Pt(IV)FL_2
A549	Lung cancer	2.5 (0.8)	20.6 (0.1)	12.7 (1.4)
HeLa	Cervical cancer	1.4 (0.3)	20.8 (2.0)	16.3 (3.1)

[a]Average of three independent experiments.

Fluorescence Cell Imaging. The most important property of Pt(IV)$(FITC)_2$ and Pt(IV)FL_2 in the present context is that they allow us to monitor cellular uptake and conversion of Pt(IV) to Pt(II) by fluorescence microscopy. To evalulate this capability, HeLa cells were incubated with 15 or 50 μM Pt(IV)FL_2 for 1, 3, 8, 24, or 48 h. During the final 30 min of incubation, a nuclear stain, Hoechst 33258, and a lysosomal stain, LysoTracker Red DND-99, were added to examine the subcellular distribution of the observed fluorescence signals. The results of the fluorescence microscopic experiments are presented in Figures 4 and S10. After a one hour treatment with 15 μM Pt(IV)FL_2, there is a pronounced intracellular green signal, a punctate pattern originating from the fluorescein chromophore. With time, the green fluorescence becomes more intense and more uniformly dispersed within the cell. Control experiments indicated that the axial ligand, FL-COOH, has very poor cell permeability and does not produce noticeable intracellular green fluorescence when incubated with cells (Figure S11). This finding leads us to conclude that the green fluorescence observed upon treatment with Pt(IV)FL_2 originates from fluorescein entering the cell as part of an intact Pt(IV) complex.

We next quantitated the time-dependent increase in intracellular fluorescein fluorescence with ImageJ software. The fluorescence intensity was averaged over 10 cells and adjusted for background for each time point. Quantitation of the fluorescence microscopy data, shown in Figure S12, reveals continuous uptake over 24 h. We are unable to derive absolute concentrations of platinum or fluorescein from the image data because the fluorescence increase is a consequence of both free and bound fluorescein. There is a lack of an internal reference for quantitation of fluorescence intensity inside cells.

Co-localization experiments showed that the green fluorescence overlaps with the lysosomal stain as a function of time. No overlap with a nuclear stain was observed. Figure 6 shows that the Pearson's coefficient,[29] a measure of the correlation of

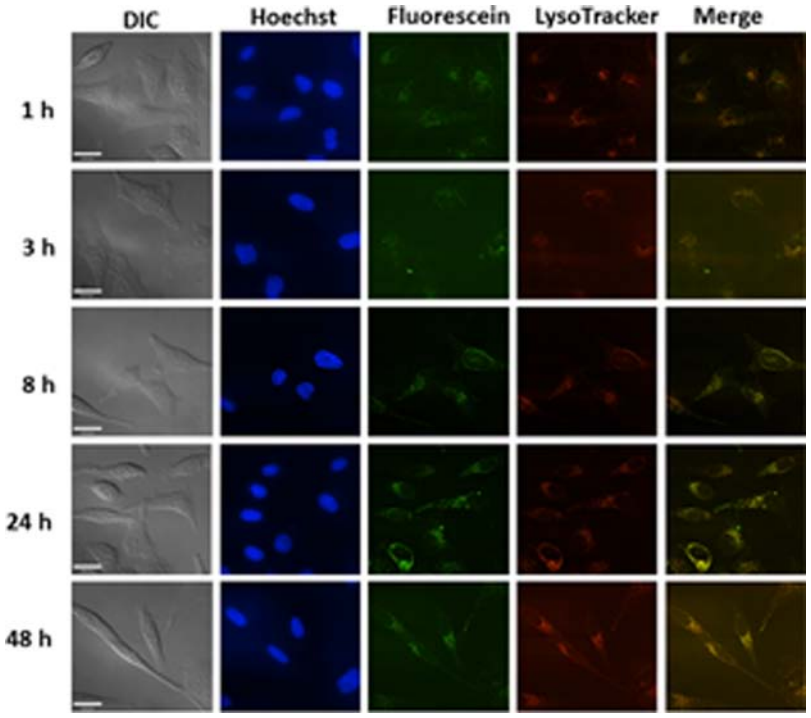

Figure 5. Fluorescence images of HeLa cells treated with 15 μM of Pt(IV)FL_2 for 1, 3, 8, 24, and 48 h. Scale bar = 26 μm. In addition, cells were incubated with Hoechst (10 μM) and LysoTracker (10 μM) for 30 min.

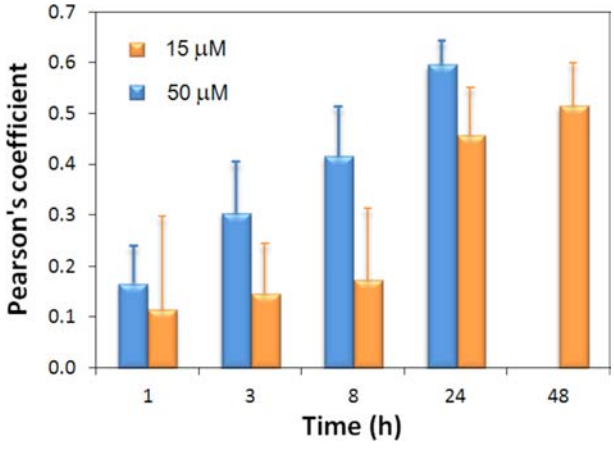

Figure 6. Pearson's coefficients of the correlation of the green fluorescein signal and the red LysoTracker signal from fluorescence images of HeLa cells treated with 15 μM and 50 μM Pt(IV)FL_2 at 1, 3, 5, 24, and 48 h. Each data point represents the average of nine regions in different cells of the same dish.

the green fluorescein signal and the red lysoTracker signal, increases during the period of exposure. We therefore propose that Pt(IV)FL_2 enters the cells, undergoes reduction, and releases its axial ligands to form an active Pt(II) species. The colocalization data suggest that, upon release from the Pt(IV) coordination sphere, the axial ligands are sequestered by lysosomes. The active Pt(II) species, on the other hand, presumably enters the nucleus and interacts with genomic DNA. In support of this mechanism, DNA from Pt(IV)FL_2 or cisplatin treated HeLa cells was isolated and the platinum content analyzed. Comparable levels of platinum, ~1 pmol/μg of DNA, were associated with DNA of cells treated with either Pt(IV)FL_2 or cisplatin (Figure S13).

Cell-Based Analysis. To understand the effect of Pt(IV)-FL_2 on cell cycle progression, DNA-flow cytometric studies were carried out. HeLa cells were treated with Pt(IV)FL_2 at the IC_{50} concentration of 15 μM for 24 or 48 h and the cell cycle distribution was analyzed by flow cytometry and compared to that of untreated cells (Figures S14–17). Twenty-four hours after addition of Pt(IV)FL_2 to the cells there was an accumulation in S phase, a 27.0% increase relative to untreated cells. Arrest at G2/M occurred after 48 h. A similar cell cycle profile was obtained following treatment with 20 μM cisplatin, a 24.6% increase in S phase after 24 h and a 63.0% in G2/M phase after 48 h. These flow cytometric data reveal that Pt(IV)FL_2 induces cellular responses similar to those induced by cisplatin, as expected for intracellular conversion to this compound.

To gain further insight into the cellular response evoked by Pt(IV)FL_2, immunoblotting analyses were carried out. Changes in expression levels of proteins associated with the DNA damage response pathway and apoptosis were monitored (Figure 7). Up-regulation of the phosphorylated form of histone H2AX (γH2AX) was detected upon incremental addition of Pt(IV)FL_2, indicative of DNA damage.[30,31] This observation is consistent with translocation of the platinum moiety to the nucleus following intracellular reduction. Cancer cells can circumvent DNA damage by one of several DNA repair mechanisms, including nucleotide excision and mismatch repair. If DNA damage is extreme, a cell that is unable to repair itself will undergo apoptosis. Apoptosis is executed by a family of cysteine proteases called caspases, which are responsible for the proteolytic cleavage of many key proteins including the nuclear enzyme poly(ADPribose) polymerase, PARP-1.[32] Caspases are activated by proteolytic processing of the inactive zymogen into the cleaved active form. Upon treatment with Pt(IV)FL_2 a clear increase in the levels of cleaved caspase-3, -7, and -9 was observed, suggesting that Pt(IV)FL_2 induces

dx.doi.org/10.1021/bc400281a | Bioconjugate Chem. 2013, 24, 1733–1740

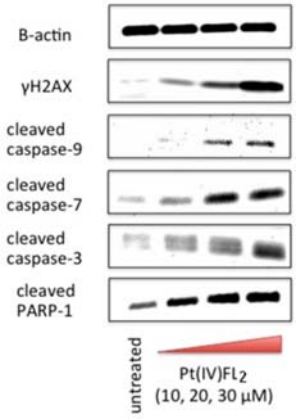

Figure 7. Analysis of protein expression in HeLa cells following 72 h incubation with Pt(IV)FL_2 at 0, 10, 20, or 30 μM.

apoptosis. Furthermore, the caspase-3 substrate, PARP-1, which is involved in DNA repair, is also cleaved upon Pt(IV)FL_2 addition, providing further evidence for apoptosis. These cellular responses are similar to those induced by cisplatin treatment. The data therefore support the hypothesis that the platinum fluorescein complexes act as prodrugs for cisplatin.

■ SUMMARY

We report two cisplatin prodrugs, Pt(IV)$(FITC)_2$ and Pt(IV)FL_2. The fluorescent ligands attached to the axial positions allow imaging of the reduction of Pt(IV). Addition of the biologically relevant reducing agent GSH results in ligand dissociation and a 5-fold turn-on in fluorescence. The Pt(IV) agents are suitable for live cell imaging as demonstrated with HeLa cells. After cell entry, Pt(IV)$(FITC)_2$ releases its axial ligands, reflecting reduction. The axial ligands accumulate in lysosomes over time, suggesting excretion through the lysosomal pathway. Intracellular reduction with axial ligand expulsion also results in formation of cytotoxic Pt(II) species. Our data are consistent with these activated species entering the nucleus, causing genomic DNA damage, and inducing apoptotic cell death. Toxicity studies indicate that both Pt(IV) complexes are potent cytotoxic agents against cervical and lung cancer cell lines, to an extent similar to that of clinically tested Pt(IV) compounds. Flow cytometry and immunoblotting experiments confirm the induction of apoptosis. In summary the two Pt(IV) compounds can be utilized to study intracellular Pt(IV) reduction and have potential as anticancer therapeutics.

■ EXPERIMENTAL PROCEDURES

General Considerations. Reactions were carried out in a fume hood in the dark. Solvents and reagents were used as received from commercial sources without further drying or purification.

Instrumentation. NMR measurements were recorded on a Bruker DPX-400 NMR spectrometer or a 400 Bruker NMR spectrometer in the Department of Chemistry Instrumentation Facility at MIT at 25 °C with either chloroform-*d* ($CDCl_3$), methanol-d_4 (CD_3OD), or *N*,*N*-dimethylformamide-d_7 (DMF-d_7) as the solvent. All chemical shifts (δ) are reported in parts per million (ppm). ^1H and ^{13}C NMR spectra were referenced internally to residual solvent peaks. ^{195}Pt NMR spectra were referenced externally to K_2PtCl_4 in D_2O (δ = −1628 ppm). IR samples were prepared as KBr pellets and Fourier transform infrared spectra were recorded with a ThermoNicolet Avatar 360 spectrophotometer using *OMNIC* software. Electrospray ionization mass spectrometry (ESI-MS) measurements were recorded on an Agilent Technologies 1100 series LC-MSD trap. Graphite furnace atomic absorption spectroscopy was carried out using a Perkin-Elmer AAnalyst600 GFAAS. All spectroscopic characterization of newly prepared Pt(IV) compounds is provided in the SI, Figures S18−S34.

Photophysical Measurements. Emission spectra were acquired with a Photon Technology International QM-4/2003 fluorimeter. 3 μL of a 5 mM stock solution of Pt(IV)$(FITC)_2$ or Pt(IV)FL_2 in DMF was diluted to 3 mL in PBS, pH 7.4, to make a 5 μM aqueous solution of Pt(IV)$(FITC)_2$ or Pt(IV)FL_2 for all fluorescence studies. Optical absorption spectra were acquired with a Cary 1E spectrophotometer. Quantum yields for fluorescence were measured using fluorescein in 0.01 M NaOH (aq) as the reference over a range of five different absorbance values with the highest absorbance being no greater than 0.1 a.u.

General Cell Culture Conditions. Human cervical cancer cells, HeLa, and lung carcinoma cells A549 were obtained from ATCC. Cells were grown at 37 °C in 5% CO_2 in a humidified incubator. All cells were grown in DMEM complemented with 10% FBS and 1% penicillin/streptomycin.

Cytotoxicity Assay. The colorimetric MTT (3-(4,5-dimethylthiazol-2-yl)-2,5-diphenyltetrazolium bromide) assay was used to evaluate the cytotoxicity of the platinum complexes. On day one, cells were plated in 96-well plates at a cell density of 1×10^3 cells/well in 100 μL of DMEM and incubated for 24 h. On day two, the medium was removed and cells were treated with medium containing platinum complexes at the following concentrations (μM): 100, 50, 25, 12.5, 6.25, 3.13, 1.56, 0.78, and 0.39. On day four, the medium was removed and cells were incubated with 90 μL of fresh medium and 10 μL of MTT solution (5 mg/mL in PBS) per well. Cells were incubated in the dark for 2 h at 37 °C. At the end of the incubation, the MTT solution was then replaced with 100 μL of DMSO per well to dissolve the formed purple crystals. The absorbance of the purple formazan was recorded with a BioTek Synergy HT multidetection microplate reader at 550 nm.

Fluorescence Microscopy. Images were acquired on a Zeiss Axiovert 200 M inverted epifluorescence microscope equipped with an EM-CCD digital camera (Hamamatsu) and an X-Cite 120 metal halide lamp (EXFO). Differential interference contrast (DIC) and fluorescence images were obtained using an oil immersion 63× objective lens, with an exposure time ranging from 250 ms to 1.75 s. Fluorescence emission was detected using Zeiss filter sets as follows: DAPI channel, Filter Set 49, excitation G 365, beamsplitter FT 395, emission BP 445/50; FITC channel, Filter Set 38 HE, excitation BP 470/40, beamsplitter FT 495, emission BP 525/50; red channel, Filter Set 43 HE, excitation BP 550/25, beamsplitter FT 570, emission BP 605/70. The microscope was operated with Volocity software (Improvision) and images were analyzed with Volocity software.

Flow Cytometry. HeLa cells (1×10^6 cells) were incubated with 16.3 μM of Pt(IV)FL_2 for 24 or 48 h at 37 °C. Cells were harvested from adherent cultures by trypsinization; floating cells were recovered from culture media to assess cell viability. Following centrifugation at 1000 rpm for 5 min, cells were washed with PBS and fixed with 70% ethanol in PBS. Fixed cells were collected by centrifugation at 2500 rpm for 3 min, washed with PBS, and centrifuged as before. Cellular pellets were resuspended in 50 μg/mL propidium iodide in PBS for

nucleic acids staining and treated with 100 μg/mL RNase. DNA content was measured on a FACSCalibur HTS-1 flow cytometer (BD Biosciences) using laser excitation at 488 nm and 10 000 events per sample were acquired. Cell cycle profiles were analyzed using the ModFit software (Verity Software House).

Western Blot Analyses. HeLa cells (5×10^5 cells) were incubated with Pt(IV)FL_2 (10, 20, and 30 μM) for 72 h at 37 °C. Cells were washed with PBS, scraped into SDS-PAGE loading buffer (64 mM Tris-HCl (pH 6.8)/9.6% glycerol/2% SDS/5% β-mercaptoethanol/0.01% Bromophenol Blue) and incubated at 95 °C for 10 min. Whole cell lysates were resolved by 4−20% sodium docecylsulphate polyacylamide gel electrophoresis (SDS-PAGE; 200 V for 1 h) followed by electro transfer to polyvinylidene fluoride membrane, PVDF (350 mA for 1 h). Membranes were blocked in 5% (w/v) nonfat milk in PBST (PBS/0.1% Tween 20) and incubated with one of the following primary antibodies: anticleaved caspase-3 (Santa Cruz Biotechnology), anticleaved caspase-7 (Cell Signaling Technology), anticleaved caspase-9 (Cell Signaling Technology), anticleaved PARP-1 (Cell Signaling Technology), antiphospho-Histone H2AX (Cell Signaling Technology), or anti-β-actin (Sigma Aldrich). After incubation with horseradish peroxidase-conjugated secondary antibodies, immune complexes were detected with the ECL detection reagent (BioRad) and analyzed using an imager fitted with a chemiluminescence filter. The untreated control sample for γH2AX expression was run in a non-contiguous lane.

Synthesis of *c,c,t*-[$Pt(NH_3)_2Cl_2(OCO(CH_2)_2NHBoc)_2$], 3. A suspension of *c,c,t*-[$PtCl_2(NH_3)_2(OH)_2$], **1**, (200 mg, 0.599 mmol) and *N*-Boc aminopropanoic acid anhydride, **2**, (1.08 g, 2.99 mmol) in DMF (2 mL) was stirred overnight at 50 °C. The resulting clear yellow solution was filtered through a pad of Celite. DMF was removed under a stream of compressed air and a small amount of methanol was used to dissolve the reaction residue. This methanol solution was added in a dropwise manner into water with stirring. A white precipitate formed immediately and was isolated by centrifugation. The final compound was obtained after washing with water and dried under vacuum. Yield: 156 mg (38.5%). mp. 183−185 °C. $^1H\{^{13}C\}$ NMR (400 MHz, DMF-d_7): δ/ppm 6.98−6.44 (m, 6H), 3.18 (q, 4H), 2.37 (t, 4H), 1.35 (s, 18H). $^{13}C\{^1H\}$ NMR (100 MHz, DMF-d_7): δ/ppm 179.89, 156.24, 78.09, 37.43, 36.71, 28.14.$^{195}Pt\{^1H\}$ NMR (86 MHz, DMF-d_7): δ/ppm 1156. IR (KBr, cm^{-1}): 3456, 3220, 2979, 2926, 1692, 1673, 1640, 1592, 1511, 1438, 1368, 1335, 1303, 1251, 1232, 1167, 1063, 971, 853, 779, 680, 560. HRMS (-): *m/z* $[M\text{-}H]^-$ calcd: 675.1316, obsd: 675.1331. Anal. Calc. for $C_{16}H_{34}N_4O_8PtCl_2$: C, 28.41; H, 5.07; N, 8.28. Found: C, 28.84; H, 5.11; N, 8.33.

Synthesis of *c,c,t*-[$Pt(NH_3)_2Cl_2(OCO(CH_2)_2NH_2)_2$]·TFA, 4·TFA. White solid *c,c,t*-[$Pt(NH_3)_2Cl_2(OCO(CH_2)_2NHBoc)_2$], **3**, (50.0 mg, 0.134 mmol) was dissolved in 1 mL of TFA/DCM (1:1, v/v) and stirred for 0.5 h at room temperature. The TFA solution was removed under a stream of compressed air. A small amount of DCM was used to redissolve the residue. The resulting solution was added in a dropwise manner to an excess of cold diethyl ether. A precipitate was formed immediately and collected by centrifugation to yield a white, hygroscopic solid, which was used directly without purification in the next step of the synthesis. Yield: 43.85 mg (68.8%). $^1H\{^{13}C\}$ NMR (400 MHz, D_2O): δ/ppm 7.83−7.20 (m, 4H), 6.40 (dd, *J* = 70.1, 50.4 Hz, 6H), 3.09 (s, 4H), 2.70 (d, *J* = 10.2 Hz, 4H). $^{13}C\{^1H\}$ NMR (100 MHz, D_2O): δ/ppm 178.99, 36.08, 32.35. $^{195}Pt\{^1H\}$ NMR (86 MHz, D_2O): δ/ppm 1070.80. HRMS (+): *m/z* $[M+H]^+$ calcd: 447.0409, obsd: 447.0401.

Synthesis of *c,c,t*-[$Pt(NH_3)_2Cl_2(OCO(CH_2)_2NH(FITC))_2$], [Pt(IV)$(FITC)_2$]. Compound **4** (44 mg, 0.097 mmol) and FITC (33 mg, 0.0850 mmol) were dissolved in 2 mL of anhydrous DMF. Upon addition of DIPEA (20 μL, 0.115 mmol), the yellow reaction mixture changed to a darker orange color and was stirred vigorously overnight at room temperature. DMF was removed under a stream of compressed air. The resulting residue was dissolved in a small amount of methanol and added in a dropwise manner into water. An orange solid was formed immediately, which was further washed with diethyl ether and water. The solids were collected by centrifugation and dried under vacuum to yield an orange colored solid. Yield 19 mg (44.7%). $^1H\{^{13}C\}$ NMR (400 MHz, DMF-d_7): δ/ppm 10.34 (s, 2H), 8.53 (s, 4H), 8.25 (s, 4H), 7.90 (d, *J* = 8.4 Hz, 2H), 7.26 (d, *J* = 8.3 Hz, 2H), 6.88 (s, 6H), 6.79−6.51 (m, 12H), 3.78 (d, *J* = 6.7 Hz, 4H), 2.62 (d, *J* = 7.1 Hz, 4H). $^{13}C\{^1H\}$NMR (100 MHz, DMF-d_7): δ/ppm 181.74, 180.61, 169.58, 160.83, 153.22, 142.60, 130.12, 129.97, 125.03, 117.32, 113.41, 111.14, 103.13, 41.56, 36.19. $^{195}Pt\{^1H\}$ NMR (86 MHz, DMF-d_7): δ/ppm 1169.9. ESI-MS (-): *m/z* $[M\text{-}H]^-$ calcd: 1253.1, obsd: 1253.6. HRMS (-):*m/z* $[M\text{-}2H]^{2-}$ calcd: 626.0459, obsd: 626.0464.

Synthesis of *c,c,t*-[$Pt(NH_3)_2Cl_2(OCO(CH_2)_2NH(FL))_2$] [Pt(IV)$FL_2$]. 57 mg (0.1207 mmol) of fluorescein NHS ester and 37 mg (0.04248 mmol) of **4** were dissolved in 1 mL of anhydrous DMF. Twenty uL (0.115 mmol) of DIPEA was subsequently added into the reaction mixture. The reaction mixture was stirred overnight at room temperature in dark. DMF was removed under a stream of compressed air. The residue was dissolved in a small amount of methanol, and the solution was added in a dropwise manner into water. Pt(IV)$(FITC)_2$ was obtained after filtration and washed with water and diethyl ether. The final product was obtained after drying in vacuum as a light yellow solid. Yield 10 mg (6.3%). $^1H\{^{13}C\}$ NMR (400 MHz, DMF-d_7): δ/ppm 8.79 (s, 1H), 8.30 (d, 1H), 8.29 (d, 1H), 6.80−6.60 (m, 8H), 3.51 (t, 2H), 2.50 (t, 2H). $^{13}C\{^1H\}$ NMR (100 MHz, DMF-d_7): δ/ppm 179.65, 168.61, 165.44, 160.51, 153.49, 152.69, 141.44, 129.83, 129.63, 129.07, 125.01, 123.06, 113.09, 110.05, 102.71, 37.18, 36.18. $^{195}Pt\{^1H\}$ NMR (86 MHz, DMF-d_7): δ/ppm 1159.27. HRMS(-): *m/z* $[M\text{-}H]^-$ calcd: 1191.1232, obsd: 1191.1247.

■ ASSOCIATED CONTENT

Supporting Information

^1H, ^{13}C, and ^{195}Pt NMR spectra of each compound, fluorescence images of cells, cell killing curves, UV−vis absorption and fluorescence spectra. This material is available free of charge via the Internet at http://pubs.acs.org.

■ AUTHOR INFORMATION

Corresponding Author

*E-mail: lippard@mit.edu. Tel: (617)253 1992. Fax: (617)253 4302.

Notes

The authors declare no competing financial interest.

■ ACKNOWLEDGMENTS

This work was supported by National Cancer Institute Grant CA034992 and by the SURF program to support undergraduate research at Caltech (JSY). Spectroscopic instrumenta-

tion at the Massachusetts Institute of Technology Department of Chemistry Instrumentation Facility is maintained with funding from National Institutes of Health Grant 1S10RR13886-01. We thank Justin J. Wilson and Timothy C. Johnstone for helpful discussions.

REFERENCES

(1) Kelland, L. (2007) The resurgence of platinum-based cancer chemotherapy. *Nat. Rev. Cancer 7*, 573−584.
(2) Wheate, N. J., Walker, S., Craig, G. E., and Oun, R. (2010) The status of platinum anticancer drugs in the clinic and in clinical trials. *Dalton Trans. 39*, 8113−8127.
(3) Siddik, Z. H. (2003) Cisplatin: mode of cytotoxic action and molecular basis of resistance. *Oncogene 22*, 7265−7279.
(4) Hall, M. D., Mellor, H. R., Callaghan, R., and Hambley, T. W. (2007) Basis for design and development of platinum(IV) anticancer complexes. *J. Med. Chem. 50*, 3403−11.
(5) Hall, M. D., Dillon, C. T., Zhang, M., Beale, P., Cai, Z., Lai, B., Stampfl, A. P. J., and Hambley, T. W. (2003) The cellular distribution and oxidation state of platinum(II) and platinum(IV) antitumour complexes in cancer cells. *J. Biol. Inorg. Chem. 8*, 726−732.
(6) Hall, M. D., and Hambley, T. W. (2002) Platinum(IV) antitumour compounds: their bioinorganic chemistry. *Coord. Chem. Rev. 232*, 49−67.
(7) Wilson, J. J., and Lippard, S. J. (2011) Synthesis, characterization, and cytotoxicity of platinum(IV) carbamate complexes. *Inorg. Chem. 50*, 3103−3115.
(8) Mukhopadhyay, S., Barnès, C. M., Haskel, A., Short, S. M., Barnes, K. R., and Lippard, S. J. (2008) Conjugated platinum(IV)-peptide complexes for targeting angiogenic tumor vasculature. *Bioconjugate Chem. 19*, 39−49.
(9) Dhar, S., Liu, Z., Thomale, J., Dai, H., and Lippard, S. J. (2008) Targeted single-wall carbon nanotube-mediated Pt(IV) prodrug delivery using folate as a homing device. *J. Am. Chem. Soc. 130*, 11467−11476.
(10) Sová, P., Mistr, A., Kroutil, A., Semerád, M., Chlubnová, H., Hrusková, V., Chládková, J., and Chládek, J. (2011) A comparative study of pharmacokinetics, urinary excretion and tissue distribution of platinum in rats following a single-dose oral administration of two platinum(IV) complexes LA-12 (OC-6-43)-bis(acetato)(1-adamantylamine)amminedichloroplatinum(IV) and satraplatin (OC-6-43)-bis(acetato)amminedichloro(cyclohexylamine)platinum(IV). *Cancer Chemother. Pharmacol. 67*, 1247−1256.
(11) Selting, K. A., Wang, X., Gustafson, D. L., Henry, C. J., Villamil, J. A., McCaw, D. L., Tate, D., Beittenmiller, M., Garnett, C., and Robertson, J. D. (2011) Evaluation of satraplatin in dogs with spontaneously occurring malignant tumors. *J. Vet. Intern. Med. 25*, 909−915.
(12) Alderden, R. A., Mellor, H. R., Modok, S., Hall, M. D., Sutton, S. R., Newville, M. G., Callaghan, R., and Hambley, T. W. (2007) Elemental tomography of cancer-cell spheroids reveals incomplete uptake of both platinum(II) and platinum(IV) complexes. *J. Am. Chem. Soc. 129*, 13400−13401.
(13) Hall, M. D., Foran, G. J., Zhang, M., Beale, P. J., and Hambley, T. W. (2003) XANES determination of the platinum oxidation state distribution in cancer cells treated with platinum(IV) anticancer agents. *J. Am. Chem. Soc. 125*, 7524−7525.
(14) Hall, M. D., Daly, H. L., Zhang, J. Z., Zhang, M., Alderden, R. A., Pursche, D., Foran, G. J., and Hambley, T. W. (2012) Quantitative measurement of the reduction of platinum(iv) complexes using X-ray absorption near-edge spectroscopy (XANES). *Metallomics 4*, 568−575.
(15) Hall, M. D., Amjadi, S., Zhang, M., Beale, P. J., and Hambley, T. W. (2004) The mechanism of action of platinum(IV) complexes in ovarian cancer cell lines. *J. Inorg. Biochem. 98*, 1614−1624.
(16) Lavis, L. D., and Raines, R. T. (2008) Bright ideas for chemical biology. *ACS Chem. Biol. 3*, 142−155.
(17) Klein, A. V., and Hambley, T. W. (2009) Platinum drug distribution in cancer cells and tumors. *Chem. Rev. 109*, 4911−4920.
(18) Wilson, J. J., and Lippard, S. J. (2012) Modulation of ligand fluorescence by the Pt(II)/Pt(IV) redox couple. *Inorg. Chim. Acta 389*, 77−84.
(19) New, E. J., Duan, R., Zhang, J. Z., and Hambley, T. W. (2009) Investigations using fluorescent ligands to monitor platinum(IV) reduction and platinum(II) reactions in cancer cells. *Dalton Trans.*, 3092−3101.
(20) Zhang, J. Z., Bonnitcha, P., Wexselblatt, E., Klein, A. V., Najajreh, Y., Gibson, D., and Hambley, T. W. (2013) Facile preparation of mono-, di- and mixed-carboxylato platinum(IV) complexes for versatile anticancer prodrug design. *Chem.—Eur. J. 19*, 1672−1676.
(21) Lakowicz, J. R. (2006) *Principles of Fluorescent Spectroscopy*, 3rd ed., Springer.
(22) Hernando, J., van der Schaaf, M., van Dijk, E. M. H. P., Sauer, M., García-Parajó, M. F., and van Hulst, N. F. (2003) Excitonic behavior of rhodamine dimers: a single-molecule study. *J. Phys. Chem. A 107*, 43−52.
(23) Runnels, L. W., and Scarlata, S. F. (1995) Theory and application of fluorescence homotransfer to melittin oligomerization. *Biophys. J. 69*, 1569−1583.
(24) Sjöback, R., Nygren, J., and Kubista, M. (1995) Absorption and fluorescence properties of fluorescein. *Spectrochim. Acta, Part A 51*, L7−L21.
(25) Meister, A. (1994) Glutathione-ascorbic acid antioxidant system in animals. *J. Biol. Chem. 269*, 9397−9400.
(26) Linster, C. L., and Van Schaftingen, E. (2007) Vitamin C. *FEBS J. 274*, 1−22.
(27) Montecinos, V., Guzmán, P., Barra, V., Villagrán, M., Muñoz-Montesino, C., Sotomayor, K., Escobar, E., Godoy, A., Mardones, L., Sotomayor, P., Guzmán, C., Vásquez, O., Gallardo, V., van Zundert, B., Bono, M. R., Oñate, S. A., Bustamante, M., Cárcamo, J. G., Rivas, C. I., and Vera, J. C. (2007) Vitamin C is an essential antioxidant that enhances survival of oxidatively stressed human vascular endothelial cells in the presence of a vast molar excess of glutathione. *J. Biol. Chem. 282*, 15506−15515.
(28) Wexselblatt, E., Yavin, E., and Gibson, D. (2013) Platinum(IV) prodrugs with haloacetato ligands in the axial positions can undergo hydrolysis under biologically relevant conditions. *Angew. Chem., Int. Ed. 125*, 6175−6178.
(29) Manders, E. M. M., Verbeek, F. J., and Aten, J. A. (1993) Measurement of co-localization of objects in dual-colour confocal images. *J. Miscrosc. 169*, 375−382.
(30) Burma, S., Chen, B. P., Murphy, M., Kurimasa, A., and Chen, D. J. (2001) ATM phosphorylates histone H2AX in response to DNA double-strand breaks. *J. Biol. Chem. 276*, 42462−42467.
(31) Rogakou, E. P., Pilch, D. R., Orr, A. H., Ivanova, V. S., and Bonner, W. M. (1998) DNA double-stranded breaks induce histone H2AX phosphorylation on serine 139. *J. Biol. Chem. 273*, 5858−5868.
(32) Hengartner, M. O. (2000) The biochemistry of apoptosis. *Nature 407*, 770−776.